Supplemental Table and Figures

Title: Inhibition of Notch1 Signaling Reduces Abdominal Aortic Aneurysm in Mice by Attenuating Macrophage-Mediated Inflammation

Authors: Chetan P. Hans, Sara N. Koenig, Nianyuan Huang, Jeeyun Cheng, Susana Beceiro, Anuradha Guggilam, Helena Kuivaniemi, Santiago Partida-Sánchez and Vidu Garg

Supplemental Table I. List of primer sequences used in qRT-PCR studies

Gene	Forward Primer	Reverse Primer
Notch1	5’-CCG TTA CAT GCA GCA GTT TC-3’	5’-AGC CAG GAT CAG TGG AGT TG-3’
Hey1	5’-TCT CAG CCT TCC CCT TTT C-3’	5’-CTT TCC CCT CCC TTG TTC TAC-3’
Mcp1	5’-CTG GAT CGG AAC CAA ATG AG-3’	5’-AAG GCA TCA CAG TCC GAG TC-3’
Il6	5’-CTA CCC CAA TTT CCA ATG CT-3’	5’-ACC ACA GTG AGG AAT GTC CA-3’
Tnf-α	5’-CCC ACT CTG ACC CCT TTA CT-3’	5’-TTT GAG TCC TTG ATG GTC GT-3’
Cxcl10	5’-CCC ACG TGT TGA GAT CAT TG-3’	5’-CAC TGG GTA AAG GGG AGT GA-3’
Vegf	5’-GGC TGC TGT AAC GAT GAA GC-3’	5’-TTA ACT CAA GCT GCC TCG C-3’
iNos	5’-CTC GGA GGT TCA CCT CAC TGT-3’	5’-TCC TG TCC AAG TGC TGC AGA-3’
Icam1	5’-GTG ATC CCT GGG CCT GGT G-3’	5’-GGA AAC GAA TAC ACG GTG ATG-3’ G
Vcam1	5’-TAC CAG CTC CCA AAA TCC TG-3’	5’-TCT GCT AAT TCC AGC CTC GT-3’
Il12	5’-GGA AGC ACG GCA GCA GAA TA-3’	5’-AAC TTG AGG GAG AAG TAG GAA TGG-3’
Arg1	5’-CTC CAA GCC AAA GTC CTT AGA G-3’	5’-AGG AGC TGT CAT TAG GGA CAT C-3’
Il10	5’-GGT TGC CAA GCC TTA TCG GA-3’	5’-ACC TGC TCC ACT GCC TTG CT-3’
Mgl1	5’-TGA GAA AGG CTT TAA GAA CTG GG-3’	5’-GAC CAC CTG TAG TGA TGT GGG-3’
Mgl2	5’-TTA GCC AAT GTG CTT AGC TGG-3’	5’-GGC CTC CAA TTC TTG AAA CCT-3’

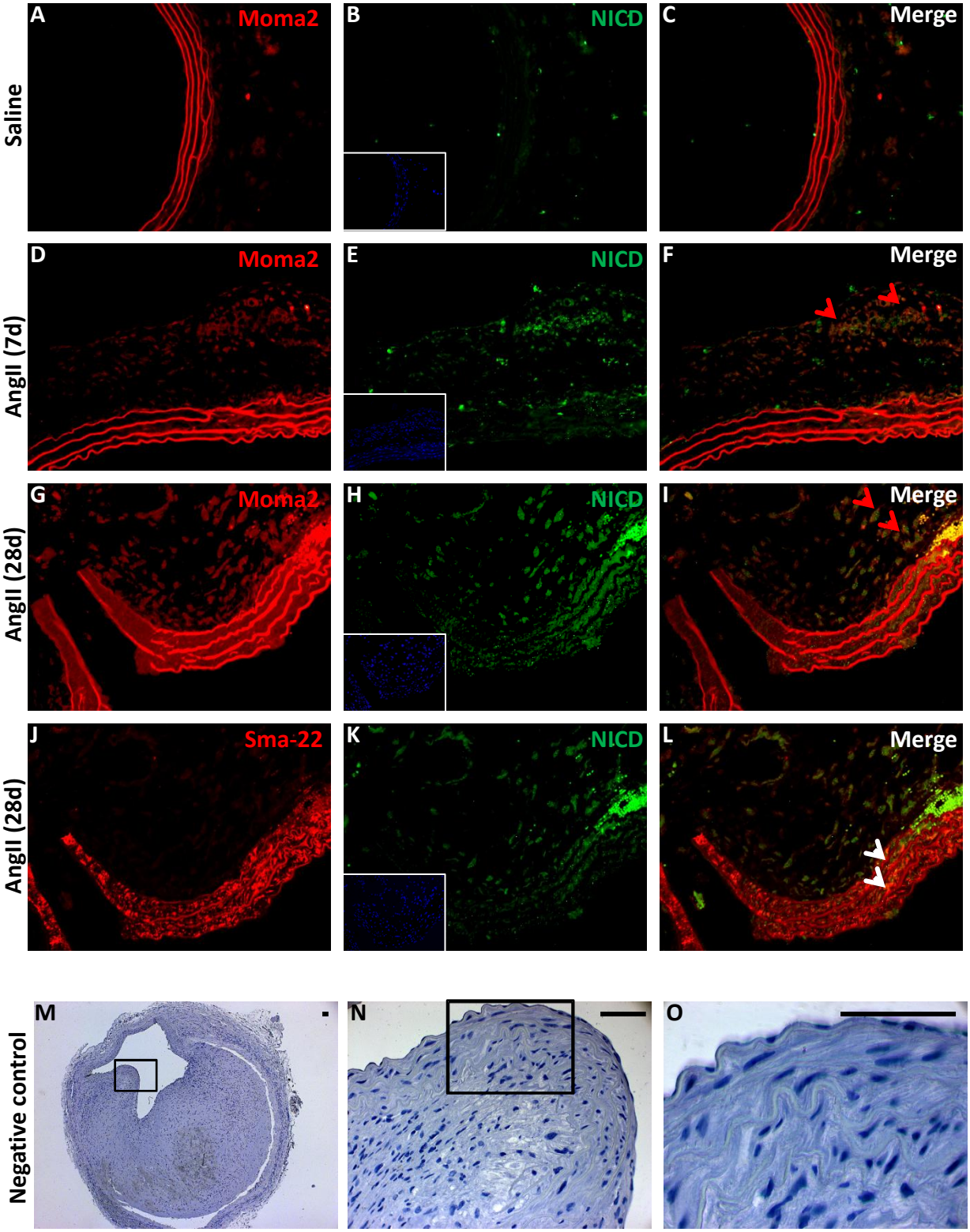

Supplemental Figure I. Increased expression of Notch1 intracellular domain localized with the macrophages in aneurysmal aorta of *Apoe*$^{-/-}$ mice. At 7 day of AngII infusion, double immunofluorescence demonstrate strong co-expression of Moma2 (red) and NICD (green) in the adventitial region of *Apoe*$^{-/-}$ mice treated with AngII (D-F) as compared to saline treated mice (A-C). At day 28, NICD staining was localized with the adventitial macrophages (I; red arrow heads) and medial SMC layer (L; white arrow heads). Of note, red staining in the aortic medial layer (A, D, G, J) corresponds to non-specific autofluorescence of elastin fibrils. Aortas from three mice were examined and representative sections are shown. Scale bar represents 50 µm. All nuclei were stained by DAPI (blue; inserts B, E, H, K). (M-O) Negative controls for NICD staining with non-specific IgG showing specificity of the NICD.

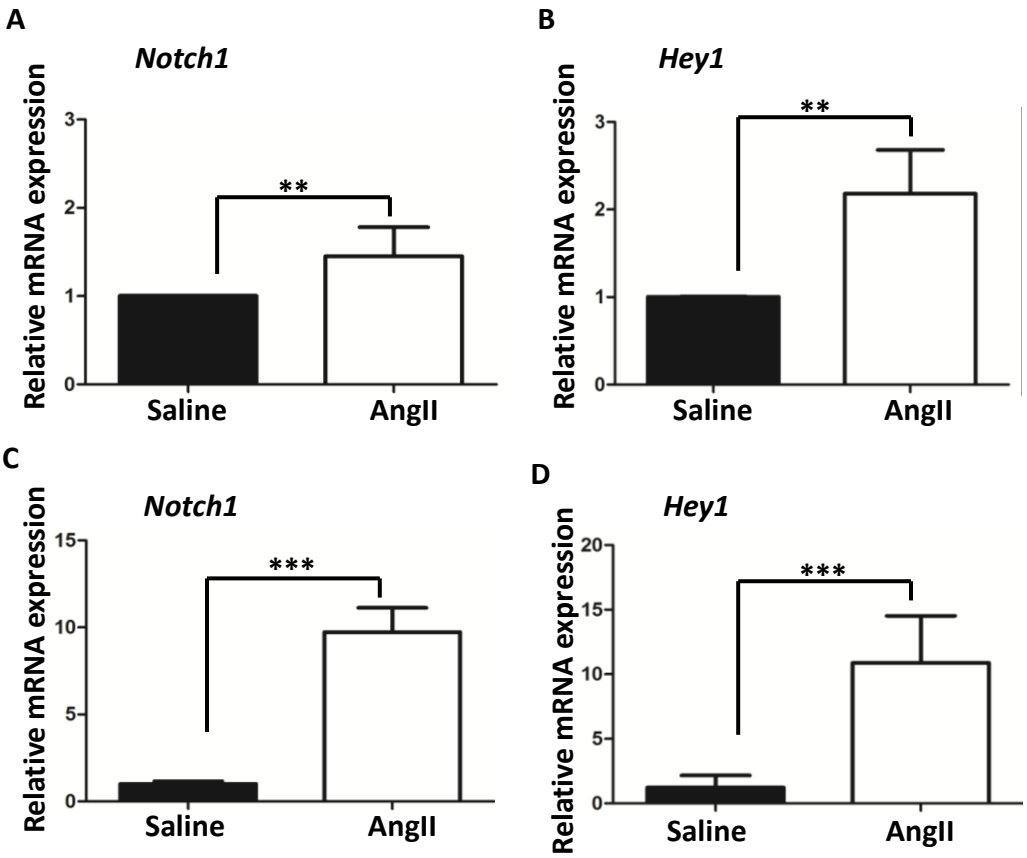

Supplemental Figure II. Increased mRNA expression of *Notch1* and its downstream *Hey1* in aneurysmal aorta of *Apoe*$^{-/-}$ mice. Quantitative real-time PCR (qRT-PCR) demonstrates increased mRNA expression of *Notch1* and *Hey1* at 7 days (A, B) and 28 days (C, D) in the abdominal aorta of AngII treated *Apoe*$^{-/-}$ mice as compared to *Apoe*$^{-/-}$ mice treated with saline (n=3). ***P<0.001; **P<0.01.

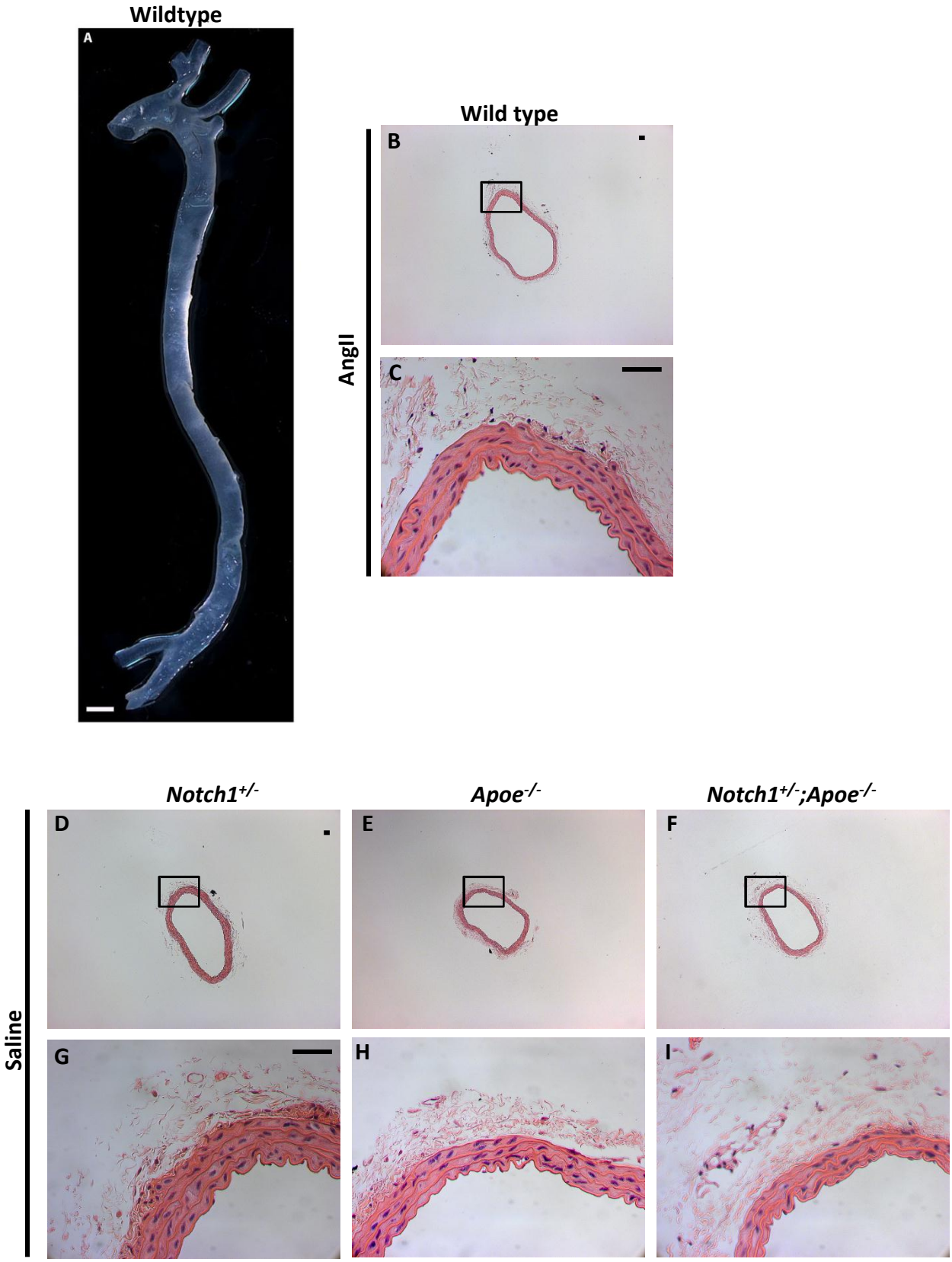

Supplemental Figure III. No evidence of AAA was found in wild-type mice treated with AngII (A- C) or *Notch1*$^{+/-}$, *Apoe*$^{-/-}$, *and Notch1*$^{+/-}$;*Apoe*$^{-/-}$ treated with saline (D-I). (n=3 mice for each group and representative images are shown). C, G, H and I are high magnification images of B, D, E and F respectively. Scale bar represents 1 mm (A) and 50 µm (B-I).

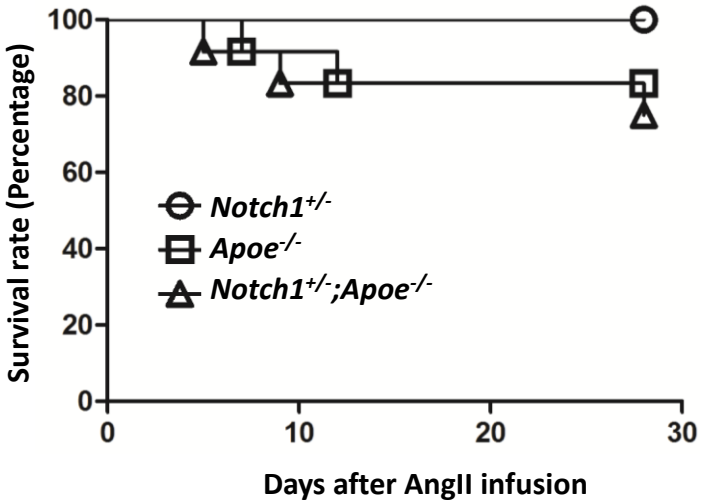

Supplemental Figure IV. *Notch1* haploinsufficiency did not affect mortality in *Apoe*$^{-/-}$ mice in response to AngII. Expectedly, about 20% mortality was observed in Apoe$^{-/-}$ mice in response to AngII. Similar mortality ratio was observed in *Notch1*$^{+/-}$*;Apoe*$^{-/-}$ mice. No mortality was observed in *Notch1*$^{+/-}$ mice on wildtype background in response to AngII.

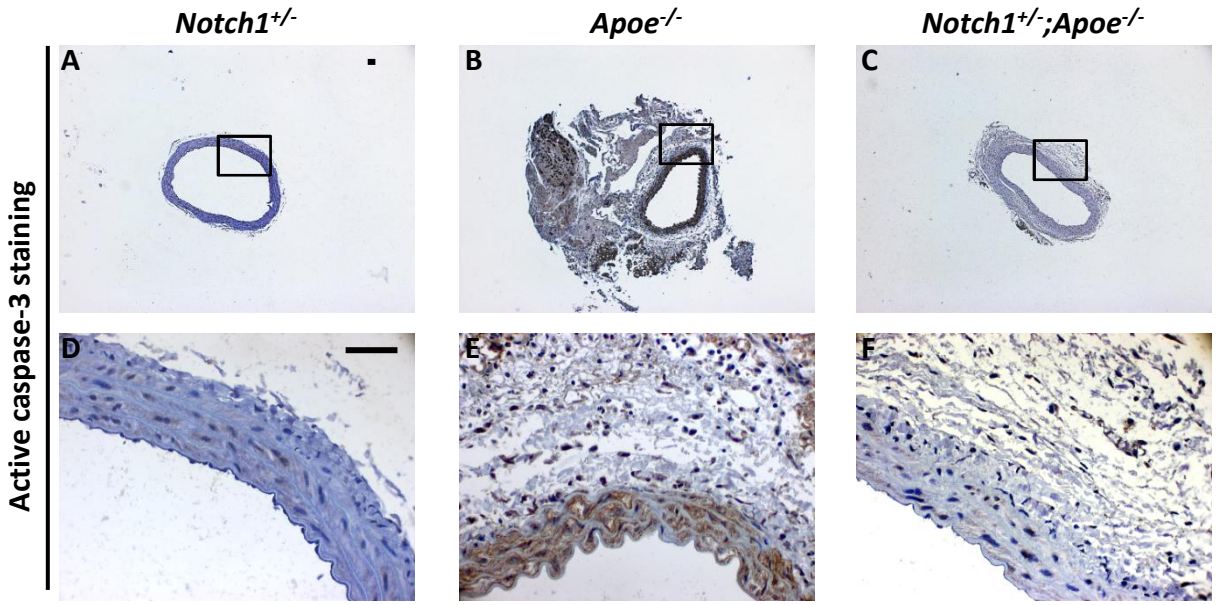

Supplemental Figure V. Decreased apoptotic cell death in the aorta of *Notch1*$^{+/-}$;*ApoE*$^{-/-}$ mice. Active caspase-3 staining (A-F) shows decreased apoptosis in all layers of the aortic wall of *Notch1*$^{+/-}$ (A, D) and *Notch1*$^{+/-}$;*Apoe*$^{-/-}$ mice (C, F) as compared to *Apoe*$^{-/-}$ mice (B, E). Scale bar represents 50 µm.

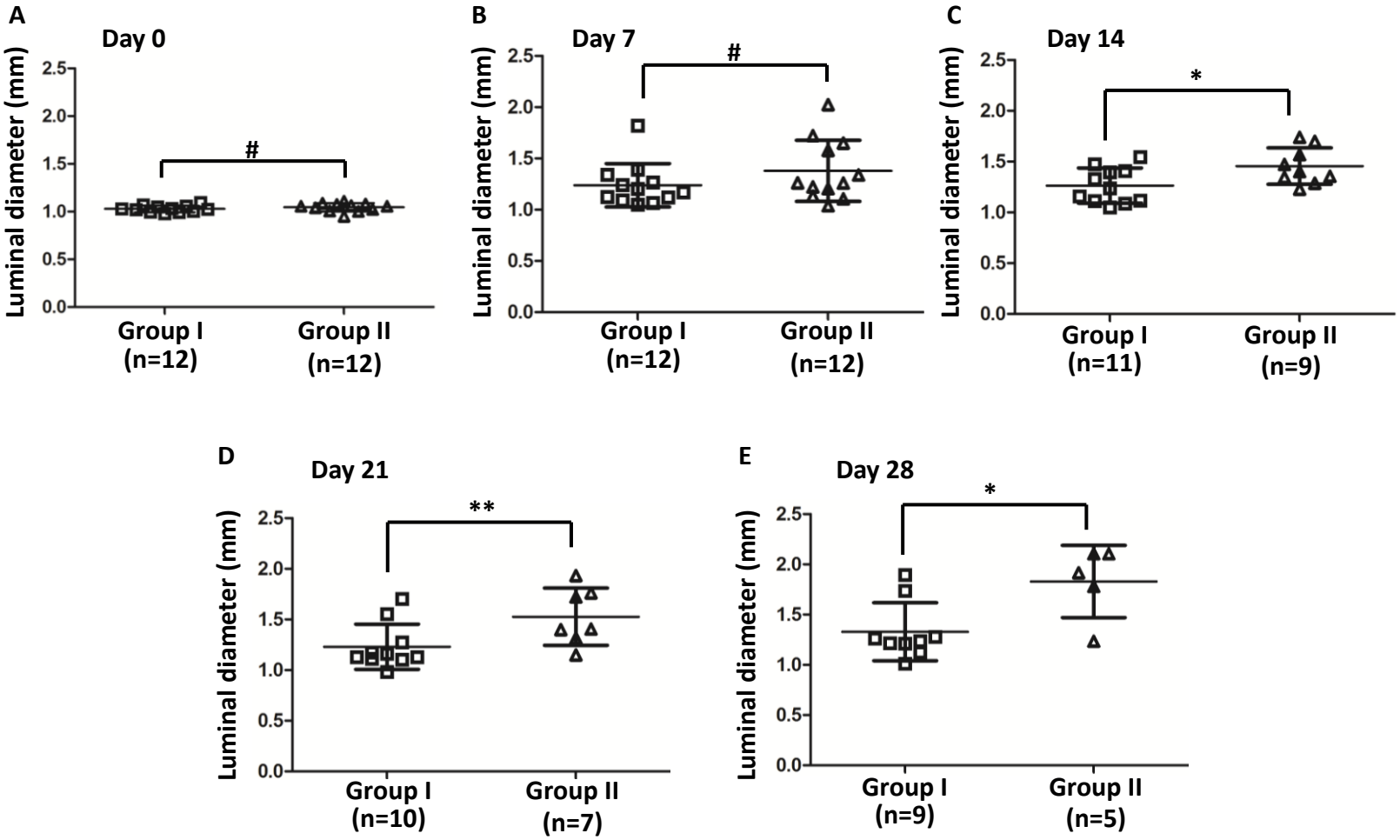

Supplemental Figure VI. *Notch1* haploinsufficiency in bone marrow-derived cells decreased aortic luminal expansion in *Apoe*$^{-/-}$ mice. The bone marrow derived cells from *Apoe*$^{-/-}$ mice increased severity of the disease in *Notch1*$^{+/-}$;*Apoe*$^{-/-}$ (Group II; *Apoe*$^{-/-}$ →*Notch1*$^{+/-}$;*Apoe*$^{-}$/-, n=12) mice as compared *Apoe*$^{-/-}$ mice which received bone marrow derived cells from *Notch1*$^{+/-}$;*Apoe*$^{-/-}$ mice (Group I; *Notch1*$^{+/-}$;*Apoe*$^{-/-}$→*Apoe*$^{-/-}$, n=12). Luminal expansion at day 0 (A), day7(B), day14 (C), day21 (D) and day28 (E) demonstrating an increase in the suprarenal luminal expansion in Group II as compared to Group I. ***P*<0.01; **P*<0.05, #non-significant.

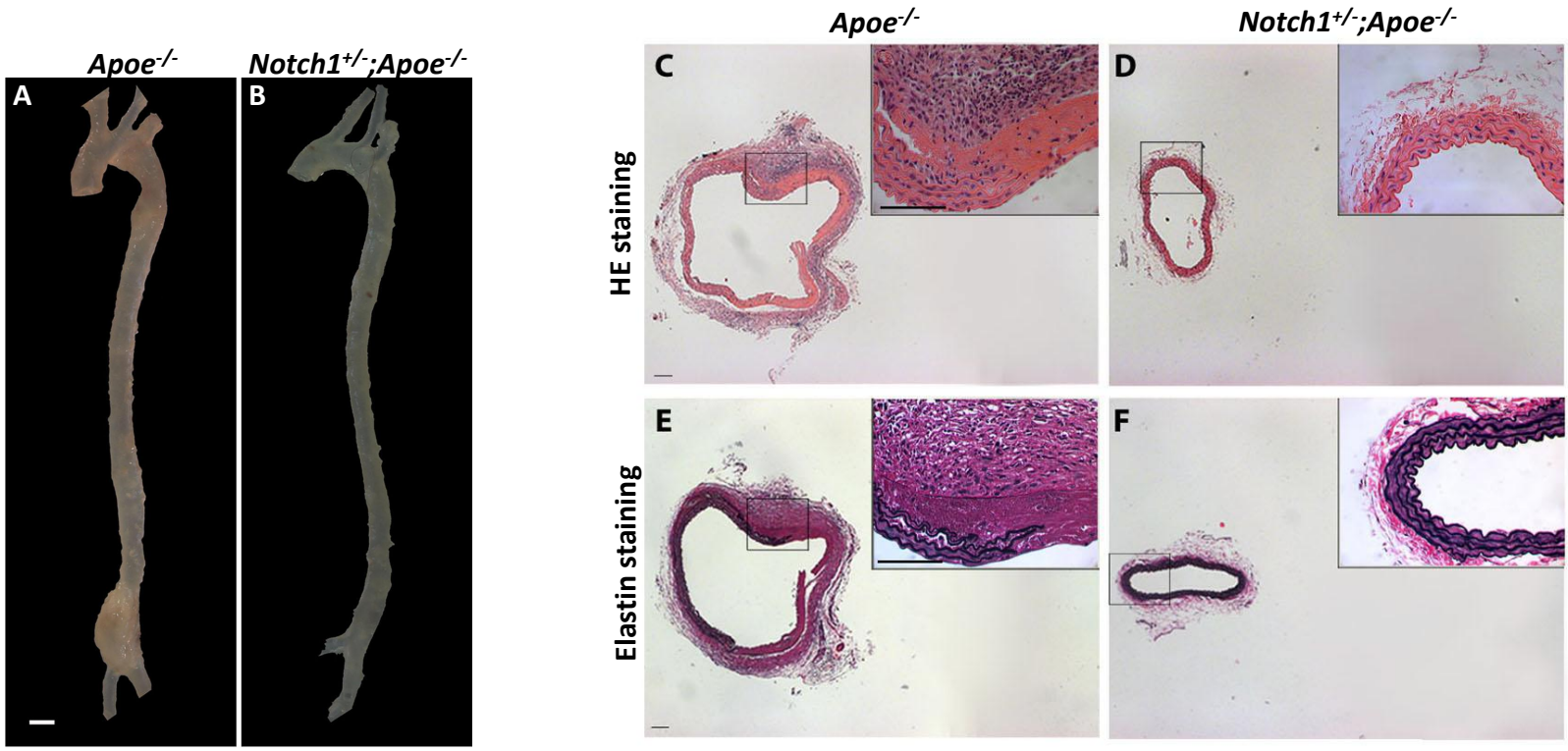

Supplemental Figure VII. *Notch1* haploinsufficiency prevents formation of AAA at day 7. Visible vascular injury was noticed in the abdominal aorta of *ApoE*$^{-/-}$ mice in response to AngII A). whereas no such evidence were found in the aorta of *Notch1*$^{+/-}$*;ApoE*$^{-/-}$ mice (B) as further confirmed by HE staining (C-D) and elastin staining (E-F). Scale bar represents 50 µm.

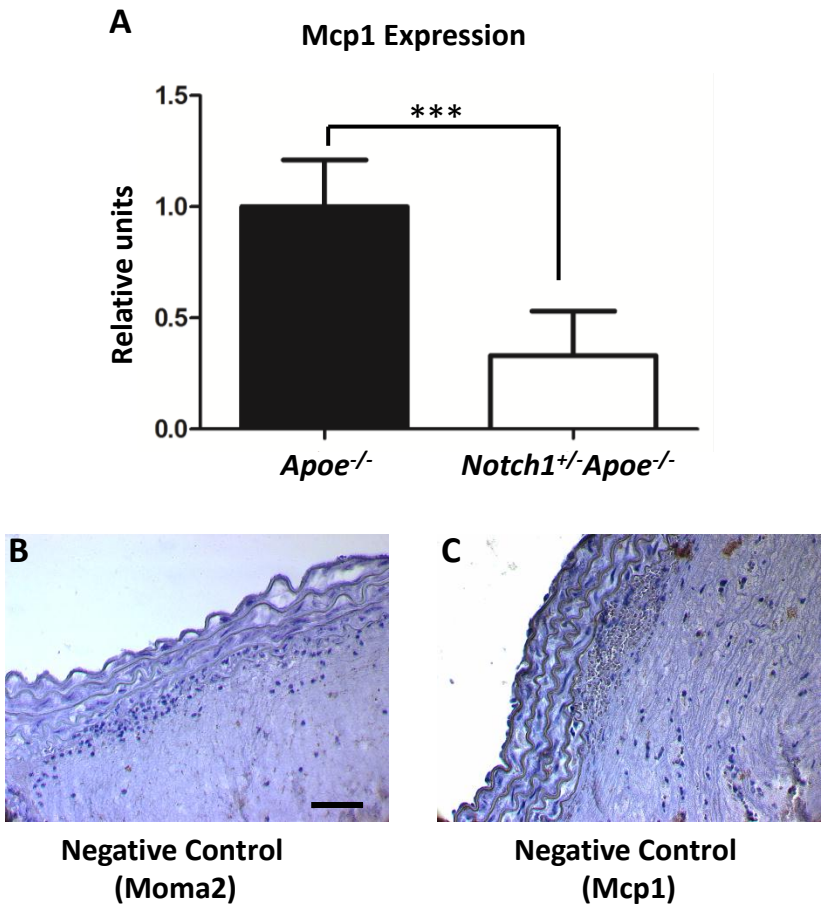

Supplemental Figure VIII. (A) Quantification of Mcp1 immunoreactivity by Image Pro-plus showing significant reduction of Mcp1 expression in *Notch1*$^{+/-}$*;ApoE*$^{-/-}$ mice as compared to *ApoE*$^{-/-}$ mice. (B,C) **Negative controls** for Moma2 and Mcp1 IHC using non-specific IgG. Means and standard deviations are shown. Scale bar represents 50 µm. ***P*<0.01.

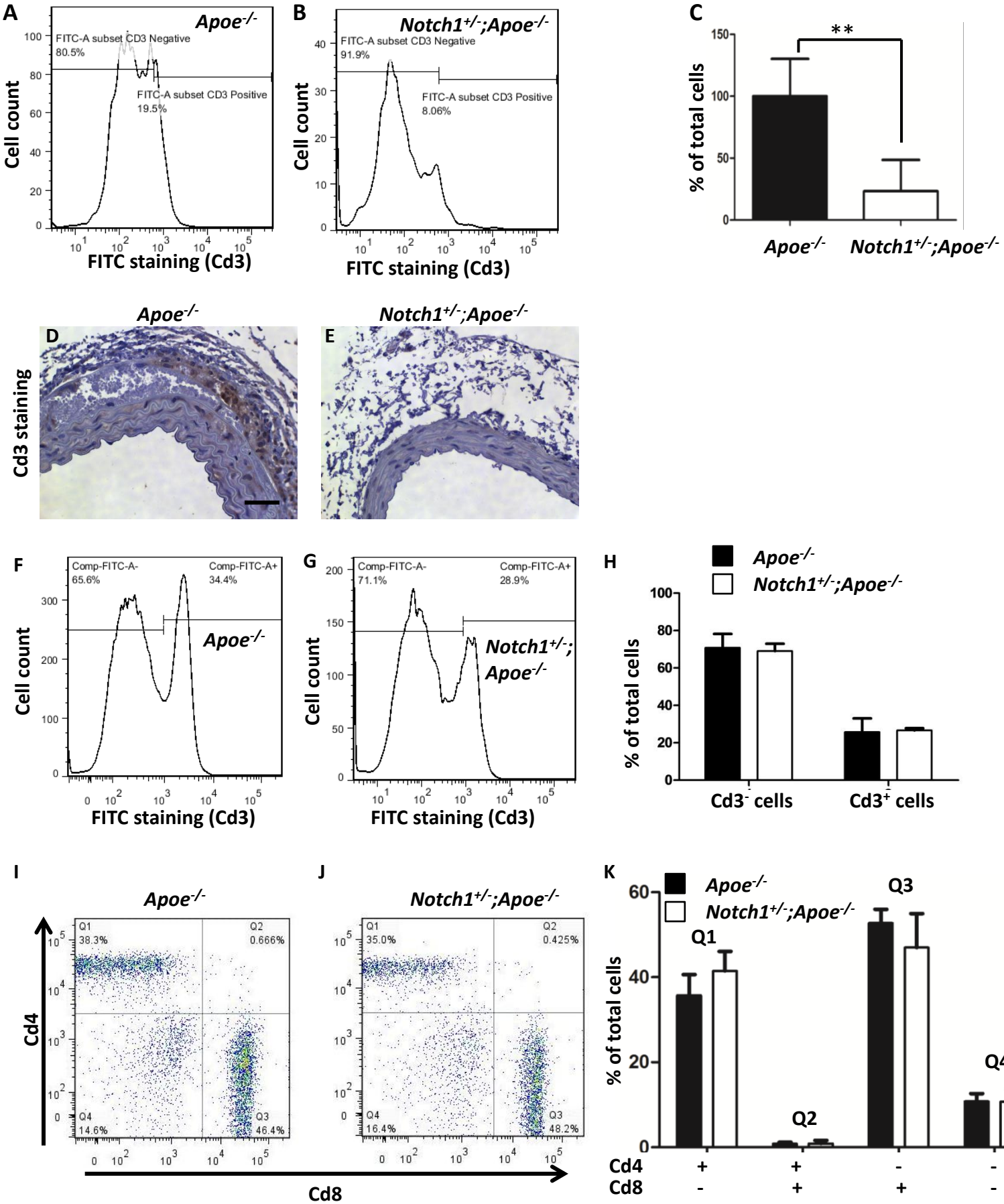

Supplemental Figure IX. *Notch1* haploinsufficiency selectively promote infiltration of Cd3⁺ cells at the site of aneurysm formation without affecting differentiation into Cd4⁺ or Cd8⁺ T cells. (A-B) FITC positive Cd3 cells at the aneurysmal site which were significantly decreased in the abdominal aorta of *Notch1*$^{+/-}$;*Apoe*$^{-/-}$ mice as shown in graph (C). (D, E) Marginal increase in Cd3 staining in the abdominal aorta of *Apoe*$^{-/-}$ mice which was absent in *Notch1*$^{+/-}$;*Apoe*$^{-/-}$ mice at day 7 of AngII infusion**.** Cd3⁺ cell population in spleen is not affected by *Notch1* haploinsufficiency (F-H). *Notch1* haploinsufficiency did not affect differentiation of Cd3⁺ lymphocytes into cytotoxic Cd4⁺ or Cd8⁺ T cells (I-K). ***P*<0.01.

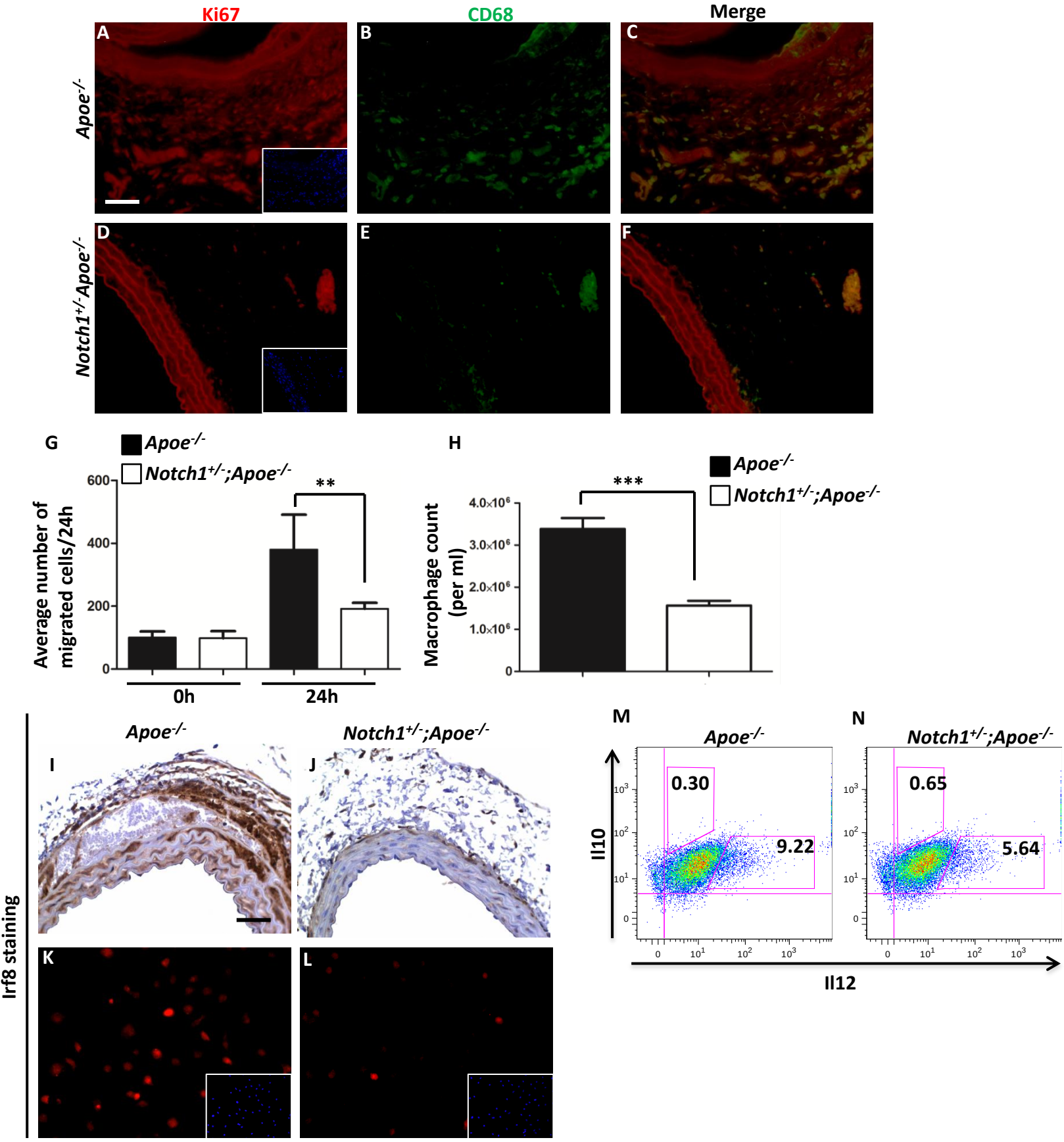

Supplemental Figure X. Effects of *Notch1* haploinsufficiency on macrophage functions. (A-F) *Notch1* haploinsufficiency decreased Ki67 positive macrophages in the abdominal aorta at day 7. (G) *Notch1* haploinsufficiency caused defects in migration of macrophages in response to chemotactic agent (FMLP; 100 nM). (H) *Notch1* haploinsufficiency decreased macrophage proliferation in the peritoneal cavity in response to thioglycollate infusion in *Apoe*$^{-/-}$ mice (n=12). (I-L) Increased expression of Notch1 dependent marker for M1 polarization (Irf8) in the aorta of *Apoe*$^{-/-}$ mice (I, J) and BMDM (K, L) in response to LPS/Ifn-γ stimulation. (M-N) FACS analysis demonstrating that *Notch1* haploinsufficiency decreased M1 polarization of macrophages in response to LPS/Ifn-γ stimulation. Scale bar represents 50μm. ***P<0.001; **P<0.01.

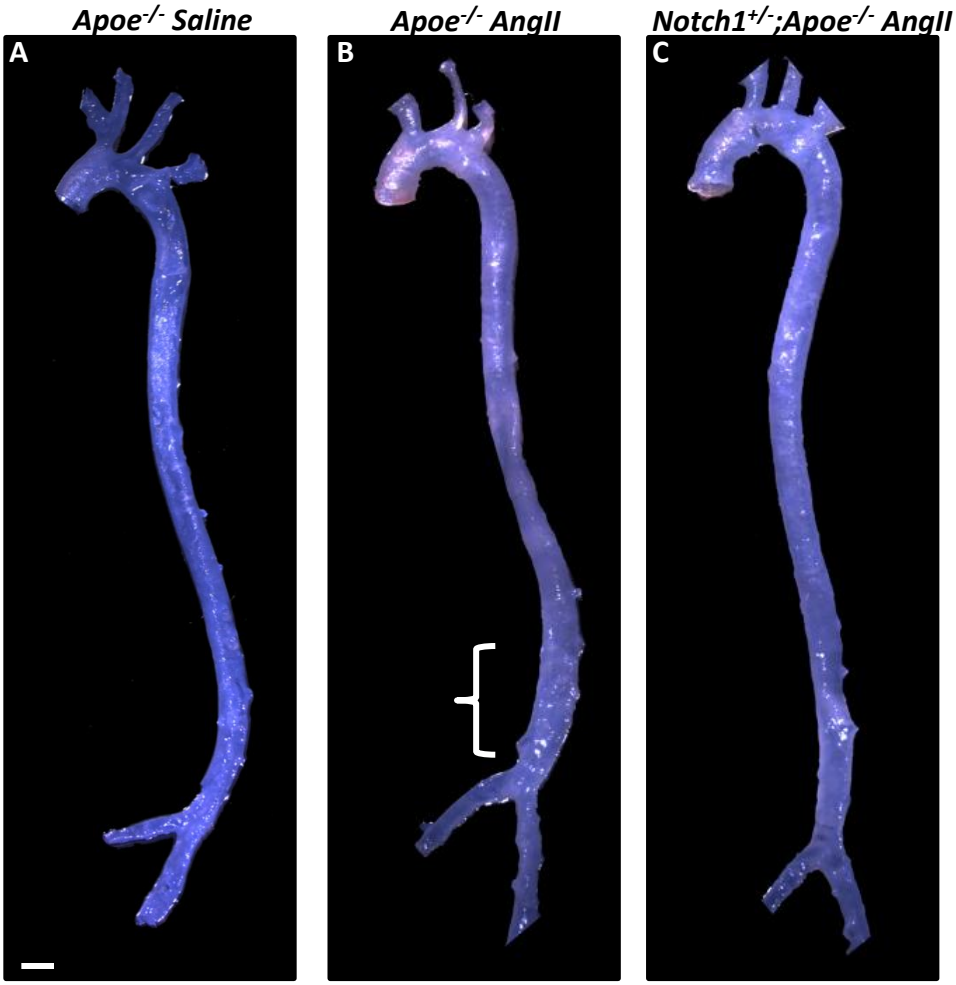

Supplemental Figure XI. ***Vascular injury in Apoe$^{-/-}$ mice at 3 days of AngII infusion*****.** Dilatation was observed in the abdominal aorta of *ApoE$^{-/-}$* mice (B) within 3 days of Ang II infusion as compared to *Notch1$^{+/-}$;ApoE$^{-/-}$* mice (C). Scale bar represents 1 mm.

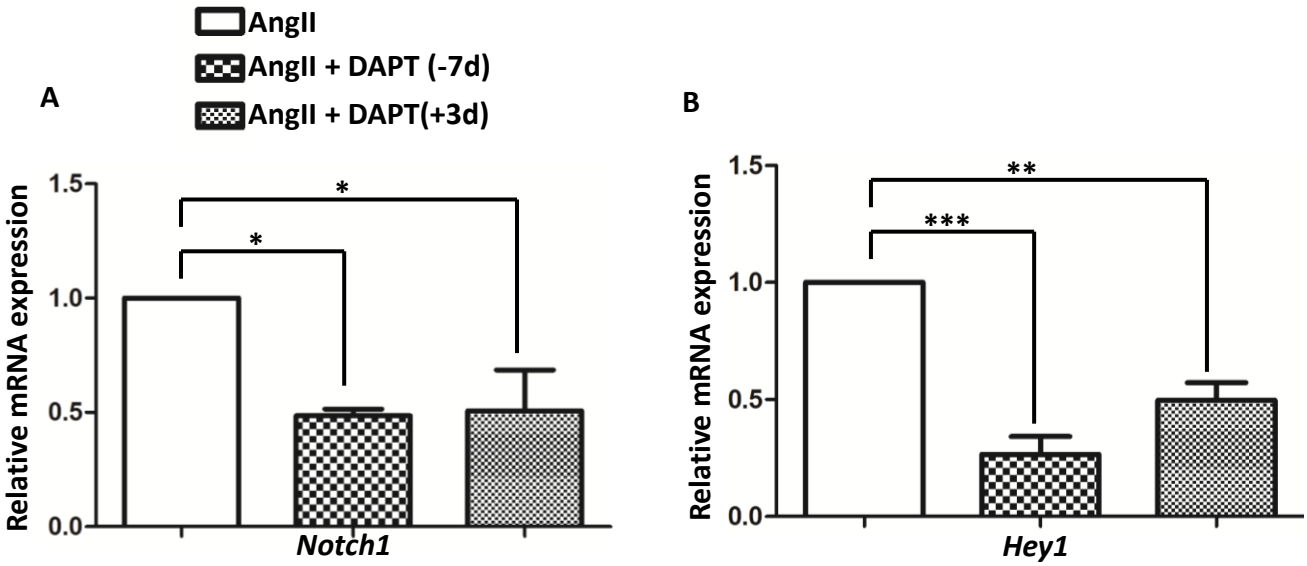

Supplemental Figure XII. ***Decreased mRNA expression of Notch1 (A) and its downstream Hey1 (B) with DAPT treatment*** *by qRT-PCR.* ****P*<0.001, ***P*<0.01, **P*<0.05.

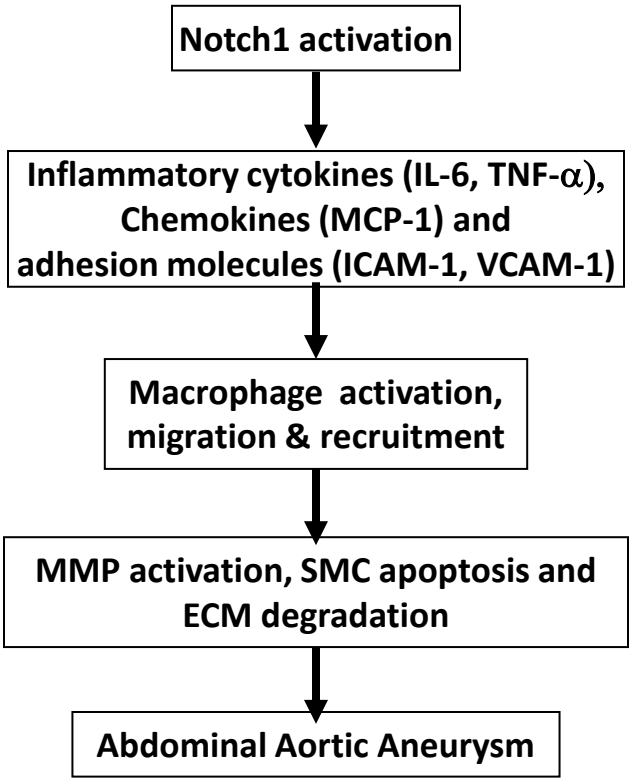

Supplemental Figure XIII. Proposed model for the involvement of Notch1 signaling in the development of AAA.

SUPPLEMENTAL METHODS

Generation of Notch1$^{+/-}$;ApoE$^{-/-}$ mice. Six to eight week old *ApoE*$^{-/-}$ female mice in a C57BL/6J background and *Notch1*$^{+/–}$ male mice (C57BL/6J background; Jackson Laboratory, Bar Harbor, ME) were crossbred to generate *Notch1*$^{+/-}$*;ApoE*$^{+/-}$ mice which were interbred to obtain *Notch1*$^{+/-}$*;ApoE*$^{-/-}$ mice. *ApoE*$^{-/-}$ mice were crossbred with *Notch1*$^{+/-}$*;ApoE*$^{-/-}$ mice to obtain *ApoE*$^{-/-}$(n=10) and *Notch1*$^{+/-}$*;ApoE*$^{-/-}$ (n=10) littermates. Mice were kept on a 12h/12h light/dark cycle with standard chow. Genotyping was performed according to the protocol from the Jackson Laboratories. Because of the variation of the extent of disease between male and female animals, only male mice were used throughout the studies. The mice (8-10 weeks old) were randomly assigned to receive saline or angiotensin II (AngII). Animal experiments were approved by Institutional Animal Care and Use Committee at the Research Institute at Nationwide Children's Hospital.

Angiotensin-II infusion and DAPT treatment. Mini osmotic pumps (Model 2004; Alzet, Cupertino, CA) containing AngII (1000 ng/min/kg) or saline were implanted subcutaneously in the neck region of anesthetized mice following standard protocol.[1] Briefly, mice were anesthetized in a closed chamber with 3% isoflurane in oxygen for 2 to 5 minutes until immobile. Each mouse was then removed, and taped on a heated (35-37°C) procedure board with 1.0-1.5% isoflurane administered via nosecone during minor surgery. Three independent experiments were performed to determine the effect of *Notch1* haploinsufficiency on the formation of AAA. The effects of pharmacologic inhibition of Notch were tested on AAA formation in two independent experiments, one of which was performed simultaneously with studies on *Notch1*$^{+/-}$*;ApoE*$^{-/-}$ mice. Mice (n=10) were injected with a Notch inhibitor, DAPT (N-

[N-(3,5-Difluorophenacetyl)-L-alanyl]-S-phenylglycine t-butyl ester (10 mg/kg dissolved in 10% ethanol, 90% corn oil), three times a week subcutaneously starting one week before the implantation of osmotic pump and continuing for an additional 28 days.[2] DAPT experiment was repeated twice, first with a set of initial study with *Apoe*$^{-/-}$ and *Notch1*$^{+/-}$*;Apoe*$^{-/-}$ mice (n=3 for each group) and second time with *Apoe*$^{-/-}$ mice alone (n=6 for *Apoe*$^{-/-}$ mice with DMSO and n=7 for *Apoe*$^{-/-}$ mice with DAPT). A portion of data from *Apoe*$^{-/-}$ mice (n=3) is shared in Figure 2 and Figure 7.

Human infrarenal aortic tissue samples. Full thickness aortic wall tissue specimens were collected from the infrarenal abdominal aorta from patients undergoing AAA repair (N = 3; Caucasian males of 67, 70 and 72 years of age) operations at the Harper University Hospital, Detroit, Michigan, USA. Non-aneurysmal infrarenal aortic samples (N = 3; Caucasian males of 53, 53 and 78 years of age) were collected at autopsies. Samples were incubated in phosphate-buffered formalin and embedded in paraffin for histological analyses.[3, 4] The collection of the human tissues was approved by the Institutional Review Board of Wayne State University, Detroit, Michigan, USA.

Blood pressure measurements, in vivo imaging and quantification of aortic width. The arterial blood pressure (BP) was measured in *ApoE*$^{-/-}$ and *Notch1*$^{+/-}$*;ApoE*$^{-/-}$ mice by the standard noninvasive tail-cuff method (BP-2000 System, Visitech Systems, Apex, NC) by a single person. The mice were allowed to acclimate to the device for 5 days and then measurements were performed during the day after 48 hours (h) of AngII infusion. Twenty BP measurements were obtained and averaged for each mouse. For *in vivo* imaging of the abdominal aorta, two dimensional (B-mode) ultrasound images were obtained at weekly intervals after the

implantation of osmotic pumps using a VisualSonics Vevo2100 imaging system (Ontario, Canada) with a mechanical transducer (MS400). After 28 days, mice were deep anesthetized with ketamine/xylazine (60 and 3 mg/kg, respectively) the aortas were dissected, fixed in 10% formalin, and maximum aortic diameters measured.

Histology and immunostaining. The abdominal aortae from the mice were embedded in paraffin and serial sections (5µm) were obtained. Sections were stained with hematoxylin and eosin (HE), elastin (Sigma, St. Louis, Mo) and immunohistochemistry (IHC) with antibodies to NICD (1:200; Abcam, Cambridge, MA), mouse monocyte-macrophage marker (MOMA-2;1:100, Abcam, Cambridge, MA), IRF8 (1:400; Abcam, Cambridge, MA), CD3 (1:400; Abcam, Cambridge, MA), MCP-1 (1:200; Abcam, Cambridge, MA) and active caspase-3 (Cell Signaling, Danvers, MA, USA), as described.[5, 6] Specificity of these antibodies was determined using non-specific IgG against the source of host species. Briefly, serial sections were deparaffinized, and antigen retrieval and blocking was performed. For IHC, Vector ABC biotin kit and Vectastain DAB substrate (Vector Laboratories, Burlingame, CA) were employed for the development of reaction and tissues were counterstained with hematoxylin. MCP-1 positive areas were quantified with Image Pro plus software using average values of positive immunostaining per microscopic field (5 fields/slide, n=3 mice/genotype)[6].

Cell Isolation and flow cytometry. Macrophages were isolated from the abdominal aorta and lymphocytes were isolated from the abdominal aorta, spleen and peripheral blood of *ApoE*$^{-/-}$ and *Notch1*$^{+/-}$*;ApoE*$^{-/-}$ mice after 7 days of AngII infusion.[7,8] Briefly, the aortas were removed from anesthetized mice (ketamine/xylazine; 60 and 3 mg/kg, respectively), minced into 3-to 4-mm pieces, and placed in 1-ml digestion solution containing 0.6 units/ml Liberase Blendzyme 3 (Roche) and 50µg/ml porcine pancreatic elastase (Sigma-Aldrich) in DMEM media. After

digestion, cells were washed in FACS buffer (0.5% BSA and 0.02% NaN_3 in DMEM) at 300 g for 5 min and subjected to FACS after staining with macrophage (CD11b and CD14). Spleens were aseptically removed and teased apart between two sterile slides. Cells were isolated and resuspended in 1 ml RBC lysis buffer (pH 7.2). After 1 min, cells were washed with RPMI 1640 medium twice and pelleted to remove cellular debris. Cells were washed and resuspended in FACS binding buffer and stained with lymphocyte (CD3, CD4, CD8) markers (eBiosciences, San Diego, CA). Blood was obtained from by cardiac puncture and erythrocytes lysed with RBC lysis solution added to the blood in a 3:1-ratio for 5 min at room temperature. Cells were centrifuged at 1,000 g for 3 min to remove the RBC lysis solution, and the leukocyte pellet was resuspended and washed in FACS binding buffer and stained with lymphocytes markers as explained. FACS studies were performed on BD (Becton Dickinson) LSRII flow cytometer with DiVa software, and data was analyzed with Flow Jo software (Ashland, OR).

Bone marrow transplantation studies and quantification of leukocytes. Using the standard validated protocol, we performed bone marrow transplantation studies on mice in which both *Apoe*$^{-/-}$ and *Notch1*$^{+/-}$*;Apoe*$^{-/-}$ mice were irradiated and repopulated with bone-marrow derived cells that were either *Notch1*$^{+/-}$*;Apoe*$^{-/-}$ or *Apoe*$^{-/-}$ mice respectively. Mice were maintained on antibiotic drinking water for two weeks before the irradiation. After optimizing the irradiation and validating the repopulation procedure, the *Apoe*$^{-/-}$ (Group I, n=12) and *Notch1*$^{+/-}$*;Apoe*$^{-/-}$ (Group II, n=12) were irradiated and reconstituted with bone marrow-derived cells harvested from *Notch1*$^{+/-}$*;Apoe*$^{-/-}$ and *Apoe*$^{-/-}$ mice, respectively. Recipient mice were irradiated with single dose of 1000 Rads from a Cesium source. Bone marrow-derived cells were obtained from the tibia and femur of donor mice (*Apoe*$^{-/-}$ and *Notch1*$^{+/-}$*;Apoe*$^{-/-}$) and were injected into the tail vein of 7-8 weeks old irradiated recipient mice ($1x10^7$ cells/ml). Two additional groups of mice

were also studied to serve as control groups: irradiated *Apoe*$^{-/-}$ mice were repopulated with bone marrow-derived cells harvested from *Apoe*$^{-/-}$ mice (Group III, n=8) and *Apoe*$^{-/-}$ mice without BMT (Group IV, n=6). Four to five weeks after the irradiation, osmotic mini-pumps containing AngII were implanted in these mice.

Macrophage migration and proliferation studies. Apoe$^{-/-}$ or *Notch1*$^{+/-}$*;Apoe*$^{-/-}$ mice (n=12) were injected intraperitoneally with 1.5 mL of 4% (wt/vol) sterile thioglycollate broth. After 4 days, peritoneal macrophages were isolated counted by Coulter counter after diluting in 5% acetic acid to lyse RBCs. RAW cells, an immortal murine macrophage cell line (264.7) were cultured following manufacturer's instructions (ATCC, Manassas, VA) Cultured macrophages were treated with Notch inhibitor (DAPT) or DMSO (control) for 6 days prior to migration and proliferation studies[9]. For the scratch assay, cells were grown as a monolayer and then scraped to create an injury. To assess proliferation, immunostaining was performed on these fixed cells with Ki67 (1:200, Abcam, Cambridge, MA) and quantified with Image Pro plus software. For chemotactic-induced migration, cells were grown in 8 μm polycarbonate filter transwell membrane plates (upper chamber) and lower chamber media was supplemented with 100 nM n-formyl-met-leu-phe, (FMLP; Sigma, St. Louis, MO). After 24 h, the cells in the lower chamber were fixed, stained with Giemsa, and counted manually. Macrophages were harvested and pooled from three mice for each experiment. Experiments were performed in quadruplicate.

Bone marrow–derived macrophages. Bone marrow-derived macrophages (BMDMs) were isolated from femurs and tibias of *Apoe*$^{-/-}$ and *Apoe*$^{-/-}$*Notch*$^{+/-}$ mice. Bone marrow was cultured in RPMI1640 supplemented with 10% FCS, 100 U/ml penicillin, 100 μg/ml streptomycin, 2 mM L-glutamine, with the addition of 20% L929-cell–conditioned medium. After 5 days of culture, cells were plated and used for experiments the next day. BMDMs were stained using biotin-

conjugated F4/80 (BM8, eBioscience) and a secondary streptavidin-Alexa Fluor 488 (Invitrogen, Carlsbad, CA) to confirm the purity of the macrophages in the population. For intracellular cytokine staining, BMDMs were stimulated with 100 ng/ml LPS E. coli O111:B4 (Sigma-Aldrich, Saint Louis, MO) and IFN-g (20 ng/ml, BioVision), or IL-4 (20 ng/ml, Biosource) for 24 hours. After treatment with the protein secretion inhibitor brefeldin A (10 μg/mL, Sigma-Aldrich) during the final 5 hours of stimulation, the cells were stained for surface markers, fixed and permeabilized using the fixation/permeabilization buffer (BD Biosciences), according to the manufacturer's instructions. IL10 was detected using a PerCP Cy5.5-conjugated antibody (JES5-16E3, eBioscience) and IL-12 (p40/p70) was detected using a APC-conjugated antibody (C15.6, BD Biosciences). Data were collected on an LSRII (BD Biosciences) and analyzed using FlowJo software (Tree Star, Ashland, OR).

RNA Isolation and qRT-PCR. The suprarenal aorta of approximately 5 mm was cut from *Apoe*$^{-/-}$ and *Notch1*$^{+/-}$*;Apoe*$^{-/-}$ mice at day 7 or 28 of AngII infusion, frozen in RNAlater, and RNA extracted using TRIzol reagent (Ambion, Austin, TX) after homogenizing tissue with TissueLyser II (Qiagen, Valencia, CA). Naïve macrophages were collected from the peritoneal cavity of *ApoE*$^{-/-}$ or *Notch1*$^{+/-}$*;ApoE*$^{-/-}$ mice (n=3; pooled from 5 mice each) by standard protocol.[6, 10] Isolated macrophages were cultured in RPMI containing 10% FCS for 3 days and then treated with 100 ng/ml LPS or diluent for 3 h in RPMI containing 1% FCS. RAW cells were pre-treated with DAPT (10 μM) or DMSO for 6 days prior to incubation with LPS. Following treatment, RAW cells and macrophages were washed and RNA extracted using RNAeasy kit (Qiagen, Valencia, CA). cDNA was synthesized using SuperScript VILO™ cDNA Synthesis Kit (Invitrogen, Carlsbad, CA) and subjected to qRT-PCR by SYBR Green RT-PCR kit (Applied Biosystems, Foster City CA) using Applied Biosystems 7500 Fast Real-Time PCR

System (Foster City CA). qRT-PCR was performed in triplicate and fold change determined by standardization to 18S rRNA. Expression levels of Notch1, Hey1 and 18S were determined by real-time PCR analysis using the TaqMan gene expression assays and TaqMan universal PCR master mix (Applied Biosystems; assay numbers, Mm_00435245, Mm_004688865 Mm_99999901 respectively) in 20 µl reaction volumes. The expression levels were standardized against 18S using the ΔΔCt method, and mean expression of the *Apoe*$^{-/-}$ mice with AngII infusion was set to 1. The primer sequences are detailed in Supplemental Table 1.

Statistical Analysis. Statistical comparisons were performed using either Student's t-test or one-way ANOVA followed by the Bonferroni's Multiple Comparison Test. GraphPad PRISM V5.0 (San Diego, CA) was used for these comparisons and a $p<0.05$ was considered significant. For the statistical analysis of actual incidence, Fisher's exact test was employed using the SAS software (Cary, NC). To analyze the BMT data for the two group comparisons at each time point, two sample t or Wilcoxon Sum Rank test was used depending on data distribution. Log rank test was used to test the null hypothesis that there is no difference between two groups in the probability of disease. For the primary outcome of the effect of AngII on the luminal expansion over time, a linear mixed effects model was used for the analysis of repeated measurement. Mean effects of AngII averaged across time and trend of change of measurement over time were compared between Group I and Group II. Differences were considered statistically significant when $P\leq0.05$ for single comparisons or after adjustment for multiple comparisons.

REFERENCES

1. Daugherty A, Manning M, Cassis L. Angiotensin ii promotes atherosclerotic lesions and aneurysms in apolipoprotein e-deficient mice. *J Clin Invest*. 2000;105:1605 - 1612.

2. Sjolund J, Johansson M, Manna S, Norin C, Pietras A, Beckman S, Nilsson E, Ljungberg B, Axelson H. Suppression of renal cell carcinoma growth by inhibition of notch signaling in vitro and in vivo. *J Clin Invest*. 2008;118:217-228.

3. Lillvis J, Erdman R, Schworer C, Golden A, Derr K, Gatalica Z, Cox L, Shen J, Vander Heide R, Lenk G, Hlavaty L, Li L, Elmore J, Franklin D, Gray J, Garvin R, Carey D, Lancaster W, Tromp G, Kuivaniemi H. Regional expression of hoxa4 along the aorta and its potential role in human abdominal aortic aneurysms. *BMC Physiology*. 2011;11:9.

4. Hinterseher I, Erdman R, Elmore JR, Stahl E, Pahl MC, Derr K, Golden A, Lillvis JH, Cindric MC, Jackson K, Bowen WD, Schworer CM, Chernousov MA, Franklin DP, Gray JL, Garvin RP, Gatalica Z, Carey DJ, Tromp G, Kuivaniemi H. Novel pathways in the pathobiology of human abdominal aortic aneurysms. *Pathobiology*. 2013;80:1-10.

5. Hans CP, Zerfaoui M, Naura AS, Catling A, Boulares AH. Differential effects of parp inhibition on vascular cell survival and acat-1 expression favouring atherosclerotic plaque stability. *Cardiovasc Res*. 2008;78:429-439.

6. Oumouna-Benachour K, Hans CP, Suzuki Y, Naura A, Datta R, Belmadani S, Fallon K, Woods C, Boulares AH. Poly(adp-ribose) polymerase inhibition reduces atherosclerotic

plaque size and promotes factors of plaque stability in apolipoprotein e-deficient mice: Effects on macrophage recruitment, nuclear factor-kappab nuclear translocation, and foam cell death. *Circulation*. 2007;115:2442-2450.

7. Tieu BC, Ju X, Lee C, Sun H, Lejeune W, Recinos A, 3rd, Brasier AR, Tilton RG. Aortic adventitial fibroblasts participate in angiotensin-induced vascular wall inflammation and remodeling. *J Vasc Res*. 2011;48:261-272.

8. Xiong W, Zhao Y, Prall A, Greiner TC, Baxter BT. Key roles of cd4+ t cells and ifn-γ in the development of abdominal aortic aneurysms in a murine model. *J Immunol*. 2004;172:2607-2612.

9. Liang CC, Park AY, Guan JL. In vitro scratch assay: A convenient and inexpensive method for analysis of cell migration in vitro. *Nat Protoc*. 2007;2:329-333.

10. Hans CP, Feng Y, Naura AS, Troxclair D, Zerfaoui M, Siddiqui D, Ju J, Kim H, Kaye AD, Matrougui K, Lazartigues E, Boulares AH. Opposing roles of parp-1 in mmp-9 and timp-2 expression and mast cell degranulation in dyslipidemic dilated cardiomyopathy. *Cardiovas Pathol*. 2011;20:e57-e68.